



University for the Common Good

Effect of GGBS on water absorption capacity and stability of superabsorbent polymers partially crosslinked with alkalis

Almeida, Fernando C.R. ; Klemm, Agnieszka J.

Published in:

Journal of Materials in Civil Engineering

DOI:

[10.1061/\(ASCE\)MT.1943-5533.0002511](https://doi.org/10.1061/(ASCE)MT.1943-5533.0002511)

Publication date:

2018

Document Version

Peer reviewed version

[Link to publication in ResearchOnline](#)

Citation for published version (Harvard):

Almeida, FCR & Klemm, AJ 2018, 'Effect of GGBS on water absorption capacity and stability of superabsorbent polymers partially crosslinked with alkalis', *Journal of Materials in Civil Engineering*, vol. 30, no. 12. [https://doi.org/10.1061/\(ASCE\)MT.1943-5533.0002511](https://doi.org/10.1061/(ASCE)MT.1943-5533.0002511)

General rights

Copyright and moral rights for the publications made accessible in the public portal are retained by the authors and/or other copyright owners and it is a condition of accessing publications that users recognise and abide by the legal requirements associated with these rights.

Take down policy

If you believe that this document breaches copyright please view our takedown policy at <https://edshare.gcu.ac.uk/id/eprint/5179> for details of how to contact us.

1 **Effect of GGBS on water absorption capacity and stability of superabsorbent polymers**
2 **partially crosslinked with alkalis**

3

4 Fernando C.R. Almeida¹, Agnieszka J. Klemm²

5

6 ¹ PhD Student, School of Engineering and Built Environment, Glasgow Caledonian University,
7 Cowcaddens Road, Glasgow, G4 0BA, United Kingdom. BSc (Eng), MSc. E-mail:
8 fernando.almeida@gcu.ac.uk (Corresponding author)

9 ² Full Professor, School of Engineering and Built Environment, Glasgow Caledonian University,
10 Cowcaddens Road, Glasgow, G4 0BA, United Kingdom. PhD, MSc (Eng), FICT, ICIQB, FHEA.
11 E-mail: a.klemm@gcu.ac.uk

12

13 **Abstract**

14 In an attempt to improve sustainability of construction and reduce Portland cement (PC) consumption,
15 supplementary cementitious materials (SCM), such as ground granulated blast furnace slag (GGBS),
16 has become a common practice. On the other hand, in order to increase durability of cementitious
17 composites, various internal curing agents, including superabsorbent polymers (SAP), are often
18 implemented. Due to their high capacity to absorb, retain and release water SAPs can provide
19 additional water for continuous hydration and lead to more homogenous microstructures. They are
20 usually neutralized by alkali metals (sodium and potassium) to increase their absorption capacities and
21 keep them stable in PC cementitious matrices. This paper discusses the applicability of SAPs in
22 blended systems. It aims to evaluate the effect of GGBS on water absorption capacity and stability of
23 three partially neutralized SAPs. SAPs swelling capacity and kinetics of the absorption, pH of binder
24 solutions over time, as well as mechanical properties of PC-GGBS matrices have been analysed. The
25 results showed that alkalis content up to 4 wt% lead to a GGBS system comparable to a stable PC
26 system. Above this limit, degradation of SAP starts to take place due to ion-exchange with GGBS
27 solution components, resulting in lower compressive strength when compared to PC matrices. Thus,
28 the excess of alkalis in SAPs network plays an important role in GGBS aqueous solution.

29

30 **Keywords:** Superabsorbent polymers (SAP), ground granulated blast-furnace slag (GGBS),
31 absorption capacity, alkalinity, cementitious materials

32 **Introduction**

33 Construction industry is constantly searching for innovations and sustainable solutions to enhance
34 environmental, structural and cost requirements. The massive production of ordinary Portland cement
35 (PC), the main cementitious material, requires consumption of high energy levels and large amounts
36 of non-renewable raw-materials. It is estimated that 5-6% of all CO₂ emissions generated by human
37 activities is derived from cement manufacture (Damineli et al. 2010; Fairbairn et al. 2010; Flower and
38 Sanjayan 2007; Huang et al. 2018; John and Zordan 2001; Pacheco-Torgal et al. 2013; Rodrigues and
39 Joekes 2011; Scrivener et al. 2016). In an attempt to mitigate this environmental issue, the use of
40 supplementary cementitious materials, such as ground granulated blast-furnace slag (GGBS), has
41 become a common construction practice (Almeida and Klemm 2018; Hooton 2008; Li 2016;
42 Lothenbach et al. 2011; Sales and Lima 2010; Siddique 2014). This by-product from pig iron
43 manufacture is a latent hydraulic material that can replace PC in contents up to 85% by weight
44 (Siddique 2014; Siddique and Bennacer 2012). However, higher GGBS contents may have serious
45 implications on concrete durability. On one hand, it can reduce permeability and increase resistance to
46 deleterious processes (e.g. chloride penetration, alkali-silica reaction and sulphate attack) (Almeida et
47 al. 2015; Divsholi et al. 2014; Klemczak and Batog 2016; Krivenko et al. 2014; Loser et al. 2010;
48 Moretti et al. 2018; Thomas 2011). On the other hand, GGBS may lead to increased carbonation rate,
49 decreased resistance to freezing/thawing and volumetric instability (Bouasker et al. 2014; Divsholi et
50 al. 2014; Ghourchian et al. 2018; Lee et al. 2006; Lothenbach et al. 2011; Lura et al. 2001; Valcuende
51 et al. 2015). Overall, cementitious properties of GGBS depend on its chemical composition, fineness,
52 glass content and alkali concentration of the reacting system (Lothenbach et al. 2011; Siddique 2014).
53 GGBS generally contains less alkali compounds than PC clinker, which leads to lower potassium and
54 sodium concentrations in blended systems over time. Hydroxide concentrations are also lower in the
55 presence of high GGBS contents. In addition to lower alkali content, pH can be decreased in GGBS
56 pore solution due to formation of reduced sulphur species, such as sulphide (HS⁻), sulphite (SO₃²⁻) and
57 thiosulfate (S₂O₃²⁻). Calcium, silicon and aluminium concentrations do not change significantly over
58 time when compared to pure PC pore solution (Vollpracht et al. 2016). Thus, especially in high levels

59 of replacement (>75 wt% of the binder), GGBS can have a strong influence on the alkalinity of
60 cementitious system.

61 The physical presence of GGBS leads to filler effect, resulting in higher reaction degree of the clinker
62 phase during early ages (dilution effect) (Lothenbach et al. 2011; Scrivener et al. 2015b). Moreover,
63 refinement of pores by GGBS increases tensile stress generated by water menisci in the capillaries
64 (Lura et al. 2001; Tazawa and Miyazawa 1995; Valcuende et al. 2015). Consequently, GGBS may
65 increase autogenous shrinkage and thus may lead to a high cracking susceptibility, triggered by self-
66 desiccation processes of cementitious materials (Bouasker et al. 2014; Jiang et al. 2014; Lee et al.
67 2006; Lothenbach et al. 2011; Lura et al. 2001; Scrivener et al. 2015a; Shen et al. 2016; Valcuende et
68 al. 2015). This cracking formation may have a severe impact on concrete durability; it establishes
69 interconnections and increases permeability, facilitating entrance of aggressive agents.

70 In order to mitigate this negative effect of autogenous shrinkage, superabsorbent polymers (SAP) can
71 be introduced as a novel admixture for internal curing (Hasholt et al. 2012; Jensen and Hansen 2002;
72 Mechtcherine et al. 2013; Mignon et al. 2017; Snoeck et al. 2015; Wehbe and Ghahremaninezhad
73 2017). SAPs are polyelectrolyte hydrogels with high ability to bind water molecules to their polymer
74 chains due to their hydrophilicity (Jensen and Hansen 2001; Mechtcherine and Reinhardt 2012). This
75 water absorption leads to formation of a swollen product that store and release water over time.

76 Hydroxides of alkali metals, usually sodium or potassium, can be considered among the primary trunk
77 chains to partially neutralize and prevent these chains from dissolving by forming a three-dimensional
78 network (Mechtcherine et al. 2015; Mechtcherine and Reinhardt 2012). Moreover, SAPs
79 modifications by alkalis as functional filler can reduce costs of their production as well as increase
80 their water absorption capacities (Li et al. 2005). For instance, in a non-modified polyacrylamide
81 network, $-\text{CONH}_2$ groups (bonded onto the polymer chains) can interact with each other by hydrogen
82 bonding. This causes an increase in crosslinking density and results in a tighter network, leading to a
83 lower polymeric expansion in water. However, when potassium or sodium salts are added into the
84 chains, these ions can weaken the formation of hydrogen bonds between $-\text{CONH}_2$ groups.
85 Consequently, it decreases the effective crosslinking density and helps to increase water absorption
86 capacity (Flory and Rehner 1943). However, there is an optimal content of alkalis to acquire the

87 maximum SAP water absorption. Values above 6.6 wt% for potassium (Chu et al. 2008) and 10 wt%
88 for sodium (Li et al. 2005) may lead to a significant reduction of water absorbency due to the
89 increased ionic concentration of external aqueous solution.

90 Moreover, as polyelectrolytes networks, SAPs can potentially exchange ions with ionic components
91 in solution (Horie et al. 2004; Jensen and Hansen 2001). The absorbable amount of liquid and the
92 storage stability, therefore, depend on SAP grading and molecular composition, as well as ions
93 dissolved in the surrounding solution (Mechtcherine et al. 2015; Siriwatwechakul et al. 2012).

94 Most of the investigations with SAPs for construction purposes has been based on hardened properties
95 of cementitious matrices, predominantly using ordinary Portland cements (Jensen and Hansen 2001;
96 Mechtcherine and Reinhardt 2012; Schröfl et al. 2017). However, their chemical interactions with
97 blended composites (for example with GGBS) are still unclear and deficient (Beushausen et al. 2014;
98 Klemm and Almeida 2018; Snoeck et al. 2015). Understanding of SAP's performance is essential in
99 decision-making process and selection of suitable type of SAP for different cementitious systems
100 (Sikora and Klemm 2015; Siriwatwechakul et al. 2012). In case of GGBS matrices, polymers with
101 higher water storage capacity and higher retention ability may display better effectiveness in
102 providing additional water for longer reactions (Almeida and Klemm 2018). This is because GGBS
103 has a lower rate of hydration compared to the clinker phases (Lothenbach et al. 2011, 2012; Scrivener
104 et al. 2015b).

105 This paper, therefore, aims to stress the importance of considering different types of cement in SAP
106 performance by assessing the effect of GGBS on water absorption capacity and stability of SAPs
107 (partially neutralized by sodium and potassium). The analyses were based on experimental data for
108 SAPs swelling capacity and kinetics of the absorption, pH of binder solutions over time, as well as
109 mechanical properties of PC-GGBS mortars.

110

111

112

113

114

115 **Experimental Programme**

116 ***Materials and mixes***

117 Three types of superabsorbent polyelectrolytes (SAP X, Y and Z) of modified polyacrylamide with
118 different water absorption capacities have been studied. They are crosslinked with different
119 concentrations of alkalis salts (sodium and potassium).

120 The polymer behaviour has been evaluated in different systems: deionized water (DI), PC and GGBS
121 filtrates, and PC-GGBS mortars. While Portland cement (PC) systems were prepared with 100% of
122 CEM I 52.5N (BS EN 197-1 2011), GGBS systems comprised 75% of ground granulated blast-
123 furnace slag (GGBS) (BS EN 15167-1 2006) and 25% of CEM I. Low reactivity of GGBS requires an
124 alkaline activator to raise pH in the vicinity of the slag, This can be provided by CH and alkali
125 hydroxides from CEM I hydration (Provis 2014; Thomas 2011). Table 1 shows the physical and
126 chemical analysis of PC and GGBS used in the experimental programme.

127 ***Table 1. Chemical and physical characterization of PC and GGBS***

128 Filtrate solutions have been prepared in the proportion of water/binder (w/b) ratio 5 (Mechtcherine et
129 al. 2018). Binders (PC and GGBS) have been immersed in deionised water for 24 h with a mechanical
130 stirrer, followed by filtration to separate binder slurry and the used filtrate solution (Mechtcherine et
131 al. 2018; Mignon et al. 2015; Schroefl et al. 2015; Snoeck et al. 2014b). Although the ionic
132 concentrations of diluted filtrates and pore solutions differ, all relevant ions for SAP sorptivity
133 analysis (i.e., Na^+ , K^+ , Ca^{2+} , OH^- and SO_4^{2-}) are well represented in filtrate solutions (Kang et al.
134 2017; Schroefl et al. 2015; Schröfl et al. 2012, 2017; Zhu et al. 2015).

135 Mortars have been produced in the proportion of w/b = 0.5, binder : fine sand = 1:2, and SAP = 0.25%
136 by binder mass. Mixing procedure was the same used in previous studies (Almeida and Klemm
137 2016a, 2018; Mechtcherine et al. 2013; Schröfl et al. 2012). Dry SAP particles were pre-blended with
138 other dry materials before adding water to the mix. Overall procedure of mortar preparation took
139 approximately 10 minutes, considering two mixing speeds (140 and 285 rotations/min). Table 2
140 shows mortars compositions used in the experimental programme.

141 ***Table 2. Mix compositions of mortars***

142

143 ***Characterization of SAPs***

144 Particle sizes of SAPs were evaluated by Laser Diffraction (Malvern Mastersizer X).

145 Shape and size were also analysed by the Scanning Electron Microscopy - SEM (Carl Zeiss EVO 50).

146 Samples were not coated and observations were carried out in high vacuum mode, accelerating
147 voltage (EHT) of 15 kV and working distance (WD) of 9 mm.

148 SAPs chemical characteristics were obtained from X-ray map data by the SEM-linked to the Energy
149 Disperse X-ray spectrometer - EDX (AZtecEnergy acquisition software with the X-MaxNand X-act
150 Silicon Drift Detector).

151 pH has been analysed (Fisher Scientific accumet AP110 pH Meter) in SAP solutions with deionised
152 water, PC filtrate and GGBS filtrate for 7 days. 0.3g of SAP has been kept in a tea-bag and immersed
153 in 100ml of solution (Schröfl et al. 2017). pH of PC and GGBS filtrates only were also evaluated.

154 For all analysis, SAP samples were tested in triplicate and stored in sealed containers under laboratory
155 conditions ($T = 21 \pm 2 \text{ }^\circ\text{C}$ and $\text{RH} = 40 \pm 5\%$).

156 Sorption characteristics were evaluated by the tea-bag method (Mechtcherine et al. 2018; Schroefl et
157 al. 2015; Schröfl et al. 2012, 2017) in deionised water (DI), PC and GGBS filtrates. Masses of SAP
158 gel were recorded at 1, 5, 10, 30, 60, 180 min, and 1, 2 and 3 days after tea-bag immersion. After that
159 period, carbonation of cement slurry solution can significantly change pH and hence affect the SAP
160 absorption behaviour, as verified by pH analysis. Before each mass record, tea-bag containing water-
161 swollen SAP was placed on a dry tissue and gently wiped for a short time (max 30 s). This was to
162 remove excess and weakly bound liquid. After weighting, the tea-bag with hydrogel was returned to
163 test solution until the next weighing step.

164 Water absorption capacities (WAC), were calculated by $\text{WAC} = (m_3 - m_2 - m_1)/m_1$, where m_1 is the
165 weight of dry SAP, m_2 is the mass of tea-bag, and m_3 is the weight of water-swollen sample. WAC
166 was expressed in grams of water per gram of dry SAP. The average WAC for three specimens per
167 solution has been used for further analysis (Mechtcherine et al. 2018; Schröfl et al. 2017).

168 A potential drawback of this method is commonly attributed to residual interparticle (capillary) liquid
169 that may remain within the samples during wiping and weighting process (Kang et al. 2017; Schröfl et
170 al. 2012, 2017). Also, the constraint from SAP particles located on the exterior could decrease the

171 absorption of SAP particles in the interior. However, recent studies showed that no decisive
172 conclusion on these issues can be drawn at this stage (Mechtcherine et al. 2018). Despite these
173 concerns, the tea-bag gravimetric method is one of the most common and widely accepted
174 quantification techniques for SAPs sorptivity assessment, and has been proved to be more practical in
175 terms of time dependent study (Mechtcherine et al. 2018; Schroefl et al. 2015; Schröfl et al. 2012,
176 2017).

177

178 ***Properties of GGBS-PC mortars***

179 Fresh and hardened properties of GGBS-PC mortars modified by SAPs have been evaluated. Flow
180 table method (BS EN 1015-3 2006) was performed in triplicate. Compressive and flexural strengths
181 tests (BS EN 1015-11 2006) were carried out after 7, 14 and 28 days. Specimens were cast into
182 prismatic moulds (160 x 40 x 40 mm³) and cured in climate chamber (T = 21 ± 2 °C and RH = 40 ±
183 5%) until the date of testing. For flexural strength test, three prims were broken providing six halves
184 which, in turn, were used for compressive strength determination (BS EN 1015-11 2006). SEM
185 micrographs were also obtained in order to evaluate porosity of GGBS mortars at 28 days (this
186 analysis followed the same procedure described in 2.2).

187

188 **Results and Analysis**

189 ***Physical and chemical characteristics of SAP***

190 Fig. 1 shows results of particle size distribution of the studied SAPs.

191 *Fig. 1. Particle size distribution of the studied SAPs*

192 Although slight differences in their distribution have been noticed (mode values for SAP Z > SAP X
193 > SAP Y), all samples had the same particle size range, predominantly between 20 and 150 µm. This
194 similar size range and irregular shape can be observed in the SEM micrographs (Fig. 2).

195 *Fig. 2. The SEM micrographs of the studied SAPs*

196 Table 3 show results of SAPs chemical composition (by EDX) obtained from the map sum spectrum
197 of all X-ray data collected.

198 *Table 3. Chemical composition of the studied SAPs by EDX analysis (by wt%)*

199 Different alkalis content (Na + K) has been found in the composition of SAPs: 4.0%, 8.8% and 12.3%
200 for SAP X, SAP Y and SAP Z, respectively. Hydroxides of alkali metals are often used for partial
201 neutralization of polyelectrolytes (SAPs) (Jensen and Hansen 2001; Kang et al. 2017; Krafcik and Erk
202 2016; Mechtcherine and Reinhardt 2012; Schröfl et al. 2017; Zhu et al. 2015). These polymers
203 dissociate in aqueous solutions and the charged molecular chains play a fundamental role in
204 determining structure, stability and interactions of various molecular assemblies (Visakh et al. 2014).
205 Fig. 3 shows pH analysis of SAP solutions over period of 7 days. Standard deviations were below 0.1
206 for all measurements. pH values for all SAP samples in DI water did not change significantly over
207 time. SAP X presented pH around 6.8, while SAP Y and Z, about 7.4 and 7.2, respectively. This
208 lower pH for SAP X is related to the lower alkali concentration compared to the other polymers.
209 Above the content shown by SAP Y in DI water (8.8%, Table 3), no significant difference was
210 observed in pH. However, in cementitious solutions, pH had a considerable drop after the third day
211 due to carbonation effect for all SAPs systems.

212 *Fig. 3. pH analysis of SAP solutions in deionised water (DI), PC and GGBS filtrates*

213 Regarding reference solution (without SAP), lower pH of GGBS filtrate compared to PC solution is
214 related to decreased alkalis and hydroxide concentrations, as well as to formation of reduced sulphur
215 species (Vollpracht et al. 2016). However, when SAPs were added to the solutions, the changes in
216 alkalinity were very dependent on the type of cementitious system. All SAP samples had a stable
217 interaction with PC filtrate; scatter of pH results was less than 0.1. In contrast, a significant change
218 could be observed when different SAPs were used in GGBS solution, especially when carbonation
219 took place. All SAP solutions showed higher pH when compared to the pure GGBS filtrate after the
220 second day (see Arrow in Fig. 3). Most likely this was due to potential formation of chemical
221 complexes between alkalis from polymers network and species from GGBS solution (as further
222 discussed in Fig. 6). In particular, SAP X showed the same behaviour as in PC system after
223 carbonation, indicating that this polymer is the most stable SAP in both cementitious systems. In turn,
224 SAP Y and Z had the highest pH values after the second day compared to both PC and GGBS
225 solutions. It suggests their higher pH-sensitivity to the changes in cementitious concentrations
226 (Mignon et al. 2014).

227 Therefore, alkalis in concentration up to 4 wt% (defined by SAP X, Table 3) were able to interact
228 with reduced sulphur species formed in GGBS aqueous solution, keeping the same pH level of a PC
229 system (after carbonation). Above this limit (for SAP Y and Z), increased pH was recorded due to the
230 excess of alkalis in SAPs composition. There may be a chemical interaction triggered by polymers ions
231 exchange (Na^+ and K^+) with ionic components of GGBS solution (as further discussed) (Horie et al.
232 2004; Jensen and Hansen 2001). This interaction was observed until the seventh day, when alkalinity
233 level of all systems seems to converge at a pH value around 10.

234

235 *SAP absorption capacity and kinetics*

236 Fig. 4 shows sorption behaviour of SAPs in DI water by tea-bag method.

237 *Fig. 4. Sorption behaviour of SAPs in DI water (left: up to 180 min; right: up to 3 days)*

238 Two stages of absorption could be observed in DI water. During the first stage, an initial intensified
239 swelling took place throughout the first 30 min. Absorption capacity values were around 240, 265 and
240 355 g/g, respectively for Z, X and Y samples, with standard deviation lower than 10 g/g. During the
241 second stage, a progressive water absorption up to SAP full capacity could be observed (around the
242 second day). This additional absorption was more pronounced for samples Y and Z; the increment
243 was in the order of 10%, 25% and 40% respectively for SAPs X, Y and Z.

244 Although SAPs Y and Z showed similar behaviour, there was a difference in their maximum
245 absorption capacities due to different alkalis contents. In this case, K^+ concentration seemed to be the
246 main responsible factor for reducing absorbency with values above 6.6 wt% (Chu et al. 2008). This
247 value is aligned with potassium contents of the studied SAPs and their respective water absorption
248 capacities: SAP Y (3.2 wt% K^+ and 440 g/g) and SAP Z (12.0 wt% K^+ and 340 g/g).

249 Moreover, SAPs sorption behaviour significantly changes when PC-GGBS systems were considered
250 (Fig. 5); not only in a substantial drop of water absorption capacity (around 10x less), but also in
251 storage and release of water.

252 *Fig. 5. Sorption behaviour of SAPs in cementitious solutions (left: up to 180 min; right: up to 3 days). Arrows in*
253 *the right graph indicate the difference between absorbency in PC and GGBS systems for all SAPs*

254 Considerable reduction in overall swelling capacity (compared to DI water) was due the presence of
255 dissolved cations in binder filtrates, especially K^+ , Na^+ , Mg^{2+} and Ca^{2+} (Mignon et al. 2015). While
256 SAP Y had the highest capacity (46 g/g), SAP X and Z had similar maximum absorption values: 39
257 and 38 g/g, respectively, with standard deviation lower than 1 g/g. All of them were reached during
258 the first 30 min in both PC-GGBS systems. After that, a considerable release took place especially for
259 SAP Y and Z; this was even more pronounced in GGBS solution.

260 In general, particles sizes have a great influence on kinetics of SAPs (Esteves 2010; Mechtcherine et
261 al. 2015), and it could potentially be observed in the test with deionised water. SAP Y, the finest
262 polymer, had the fastest water intake, while SAPs X and Z had similar absorption in the first 10 min.
263 However, considering the small range between the particle sizes (Fig. 1), the effect of SAP diameters
264 was not noted in cementitious solutions (Fig. 5). When both PC and GGBS filtrates are considered,
265 SAP Z (with the largest particles) showed the fastest water absorption, contradicting the concept of
266 the finer particle the faster absorption. Its faster absorptivity may be related to its high alkali content
267 that increases charge concentration of the system. The high amount of K^+ in SAP Z increases osmotic
268 pressure difference between the polymer and the cementitious aqueous solutions, which results in a
269 faster water absorbency (Li et al. 2005). Thus, particularly for this study, it seems that the type of
270 polymer in terms of chemical composition was the main factor influencing sorption characteristics of
271 the studied SAPs in cementitious systems.

272 In PC solution, after the max WAC is reached, SAPs Y and Z started to release water: up to the first
273 day for SAP Y, and up to the second day for SAP Z. Thereafter, both SAPs had the ability to re-
274 absorb water up to its max WAC (reached during the first 30 min).

275 However, in GGBS system, this initial release of water was higher (for both SAPs) and no further
276 absorption was noted. This may indicate degradation of SAP Y and Z, due to the loss of their stability
277 of water retention.

278 In turn, SAP X, although had a slight increment of absorbency in PC solution, it kept nearly unaltered
279 over time in GGBS system. It indicates higher stability of this polymer in both cementitious solutions.
280 Thus, its alkali content of 4 wt% may rule the stability of the polymer in GGBS systems, which seems

281 enough to bind with reduced sulphur species. Above this concentration, exchange of ions between
282 polymers and aqueous solutions may lead to low ability to store water.

283 This effect of SAP instability was described as polymer degradation (Mignon et al. 2014, 2015;
284 Tachibana et al. 2017). It means a decrease of network integrity; chain junction knots can hydrolyse
285 resulting in a drastic swelling reduction. It has been reported that solutions with higher cation
286 concentrations (especially divalent cations) are concomitant with reduced hydrolysis (Dho and Choi
287 1995; Mignon et al. 2015). Indeed, desorption capacity was even higher in GGBS system (with
288 reduced Ca^{2+} content, see Table 1), indicating greater sensitivity of SAPs Y and Z. The difference
289 between absorption/storage capacities in PC and GGBS systems was clearly higher for these SAPs
290 (when compared to SAP X) during the first three days (see arrows in Fig. 5); almost no difference was
291 noted for SAP X during the first 180 min of test.

292 These results are aligned with pH analysis (Fig. 3) where SAP Y and Z have also showed instability in
293 GGBS system, most likely due to their high alkalinity (Table 3). Addition of K^+ and Na^+ in SAPs
294 chains have the ability to weaken hydrogen bonds formation and, in consequence, facilitate (or
295 induce) complex bonds between the polymeric network and metal ions from cementitious solutions.
296 Moreover, the presence of S^{2-} in SAP X could indicate that this ion contributes to greater polymer
297 stabilization by forming disulphide bonds. These are very strong bonds able to hold polymers in their
298 respective conformations, and therefore, play an important role in their folding and stability (Brandt et
299 al. 2017). Disulphide bonds can only be cleaved by external stimulus, such as oxidation-reduction
300 potential (Tachibana et al. 2017). However, as SAP Y also contains sulphide, it is suggested that high
301 alkali content seems to be the main responsible factor for SAP Y and Z degradations in GGBS
302 systems.

303 Surrounding cementitious solutions with univalent cations (e.g. K^+ and Na^+) have the easiest
304 interaction with a crosslinked potassium/sodium hydrophilic network, followed by mediums with
305 divalent (Mg^{2+} and Ca^{2+}) and then trivalent (Al^{3+} and Fe^{3+}) cations. Thus, water absorption capacity of
306 SAP and its storage stability decrease with the increase of ionic strength of external saline solution;
307 the stronger salt ions bonds (from solution), the lower is the effect on the charge of SAP chain. Thus,

308 the ease of interaction is in the following order: $K^+ = Na^+ > Mg^{2+} > Ca^{2+} > Al^{3+} > Fe^{3+}$ (Chu et al.
309 2008).

310 It is worth noting that potassium/sodium modified SAPs are more likely to interact with Mg^{2+} than
311 with Ca^{2+} from cementitious solutions. This ionic preference can explain how SAPs Y and Z had
312 more unstable performances in GGBS systems compared to PC solutions; MgO content is 4.4 times
313 higher in GGBS than PC (Table 1). The presence of divalent cations form strong complexes with the
314 polymer chain and act as additional cross-linker, resulting in low swelling degree (Mignon et al.
315 2015). Al_2O_3 can also contribute to form complex bonds with those SAPs in GGBS environments,
316 since Ca^{+2} concentration is lower than PC and this ion is also “disputed” with carbonation reactions
317 (observed in both PC-GGBS filtrates). Univalent cations content seems to be very low compared to
318 other elements, especially in GGBS systems (lower than PC’s), resulting in negligible interactions
319 with SAPs. Such interaction is schematically represented in Fig. 6, particularly with Mg^{2+} and Al^{3+}
320 ions.

321 *Fig. 6. Polyacrylamide structures and their modifications (adapted from Chu et al. 2008)*

322 Therefore, SAP X is more stable and less sensitive to the type of cement, in particular in PC-GGBS
323 matrices. It seems that there is a certain limit of alkali content in SAPs of around 4 wt% that can retain
324 stability of GGBS system similar to PC solution. These alkalis can interact with reduced sulphur
325 species (HS^- , SO_3^{2-} and $S_2O_3^{2-}$) formed in GGBS aqueous solution that generally are not found in PC
326 systems (due to its higher alkali concentration compared to GGBS). Consequently, SAP’s alkalis (up
327 to 4 wt%) combined with GGBS reduced sulphur ions keep SAP-GGBS system stable similarly to the
328 SAP-PC system.

329 Above this limit, additionally to this chemical interaction, ion-exchange can take place between
330 “extra” SAP alkalis (Na^+ and K^+) and additional ions of Mg^{2+} and Al^{3+} from aqueous solution
331 (compared to the amount of these ions in PC system). This ion-exchange can lead, however, to SAPs
332 degradation and hence, reducing their stability in water retention.

333

334

335

336 *Effect of SAPs on GGBS-PC mortars*

337 Fig. 7 compares results of consistency of fresh mortars modified by SAPs with their respective
338 reference samples. Overall, all SAPs decreased flowability for both PC-GGBS systems (Filho et al.
339 2012).

340 *Fig. 7. Flow-table results of PC-GGBS mortars modified by SAPs*

341 Duration of flow-table test had a significant impact on the results. SAP X had a slightly lower
342 absorption rate compared to SAP Y and Z in the first 30 min (Fig. 5). In consequence, this polymer X
343 resulted in the highest flow values among SAP mortars, even though its final WAC was between Y
344 and Z samples in cementitious filtrate solutions. Moreover, addition of sand can imply a “dilution
345 effect” of PC-GGBS ions. Sorption behaviour of SAPs obtained in mortars (by flow-table test) was
346 similar to that in DI water (by tea-bag method after the first day). The use of mechanical mixer for
347 mortars preparation could have stimulated SAPs to reach their maximum WAC during mixing/casting
348 procedures. Thus, SAP X had the lowest absorption capacity in mortars, as in DI water.

349 Results of mortars compressive strength over the first month are shown in Fig. 8. Overall, GGBS has
350 reduced compressive strength for all samples due to its slower hydration rate. As reported by
351 Lothenbach et al. (2012) about 90% of GGBS hydrated during 3.5 years. Moreover, overall porosity
352 of PC-GGBS matrices is higher due to the lower total volume of C-S-H formed by GGBS when
353 compared to pure PC systems (Lothenbach et al. 2011).

354 *Fig. 8. Compressive strength results of PC-GGBS mortars modified by SAPs*

355 The type of SAP had a greater impact than the type of binder. In PC mortars, all compressive strength
356 values were comparable. In contrast, when GGBS was considered, a clear pattern was observed for all
357 ages: while SAP X was very similar to the reference sample, SAP Y and Z had the lowest strength
358 values during the first 28 days. In particular for SAP Y, whose higher WAC could have aggravated
359 mechanical properties of mortars. This is because greater swelling rate may lead to macro-pore
360 formation in the hardened state (Almeida and Klemm 2018; Farzaniyan et al. 2016; Farzaniyan and
361 Ghahremaninezhad 2017; Pourjavadi et al. 2013; Schröfl et al. 2012; Snoeck et al. 2014a).

362 Their lower compressive strength results (for SAP Y and Z) may be also related to the instability in
363 GGBS systems. Both SAPs have not showed a reliable capacity to store water for longer periods (Fig.

364 5). Thus, after polymer collapses, SAPs left behind larger pores, which could not be refilled with
365 hydration products due to the lack of water. It is very likely that this collapse of SAP took place in the
366 first week of hydration, since the pattern was the same for all studied ages.

367 In summary, reduction in compressive strength for SAP Y and Z mortars (during the first month) can
368 be related to two main concomitant factors: larger pores formation and low ability to water retention.
369 Their macropores are even larger than those formed by SAP X, due to their higher WAC (collapsed
370 SAPs). Once these larger pores are formed, there is not enough water to induce longer GGBS
371 reactions, and hence, to refill those macropores with later hydration products. This outcome is aligned
372 with previous detailed studies on microstructure alteration of SAP-PC-GGBS mortars (Almeida and
373 Klemm 2016b, 2017, 2018). Fig. 9 illustrates these larger macropores formation at 28 days, especially
374 for SAPs Y and Z mortars.

375 *Fig. 9. SEM micrographs of GGBS mortars at 28 days (indication of larger pores in samples modified by SAP Y*
376 *and SAP Z)*

377 Therefore, SAPs chemical composition, in particular its potassium/sodium salt modifications, has a
378 significant influence on compressive strength. This is even more evident in GGBS matrices.

379 Regarding flexural strength, no significant difference in the overall pattern could be identified
380 between specimens modified by SAPs (Fig. 10).

381 *Fig. 10. Flexural strength results of PC-GGBS mortars modified by SAPs*

382 However, at 28 days, SAP-GGBS mortars showed less variation in results than SAP-PC mortars when
383 compared to their respective reference samples. This could be explained by the sensitiveness of the
384 test to smaller pores. GGBS refines capillaries and leads to a denser structure of micropores (below 50
385 nm for high GGBS content) (Almeida and Klemm 2017, 2018; Li et al. 2010). Thus, results of
386 flexural strength for GGBS mortars are more similar to each other, regardless the addition of SAP. In
387 contrast, a slight reduction in strength can be observed in some PC mortars modified by SAP.

388 Thus, the type of SAP had a considerable effect on compressive strength of GGBS mortars up to 28
389 days. However, no significant impact was observed on flexural strength, especially for high GGBS
390 contents.

391

392 **Conclusions**

393 Based on the experimental data, the following can be concluded:

- 394 • Behaviour of SAPs with alkali content around 4 wt% in GGBS systems is similar to a stable
395 PC system. Up to this concentration, sodium/potassium ions may bind with reduced sulphur
396 species formed in GGBS solutions. This combination is able to retain pH of GGBS solution at
397 the same level as pH of the PC solution after carbonation;
- 398 • SAPs with alkalis contents above 4 wt% lead to increased polymer degradation in GGBS
399 solution, characterized by loss of water storage capacity and increased pH. The excess of
400 alkalis may lead to ion-exchange between potassium/sodium in SAP and di- and trivalent ions
401 in GGBS. It is most likely due to the higher contents of MgO and Al₂O₃;
- 402 • Absorption capacity of SAPs changes according to type of cementitious environment.
403 Aggregates can also lead to a “dilution effect” of PC-GGBS ions by its addition to the mix. In
404 this case, SAPs sorption patterns are more similar to those obtained for DI water than for PC-
405 GGBS filtrate solutions;
- 406 • SAP instability, due to excess of alkalis in the polymer network, may affect mechanical
407 properties of GGBS matrices, in particular compressive strength. Its limited ability to store
408 water for longer periods results in formation of larger pores that cannot be filled with later
409 GGBS products (due to slower reaction of slag compared to clinker phases);
- 410 • SAP X, with 4 wt% of alkalis crosslink in its composition, showed itself to be the most stable
411 and suitable for both cementitious systems studied. It results in formation of cementitious
412 matrices with similar compressive strength to the reference samples.

413

414 Therefore, although the studied SAPs have been designed for a stable performance in Portland cement
415 systems, the excess of alkalis in SAPs compositions leads to chemical interactions with GGBS
416 aqueous solution (with reduced pH) and hence, to instability of the polymeric network.

417

418

419 **Acknowledgements**

420 The authors acknowledge CNPq (National Council for Scientific and Technological Development –
421 Brazil) for the financial support (Grant Number: 204097/2014-2), and BASF for SAPs supply.

422

423 **References**

424 Almeida, F. C. R., and Klemm, A. J. (2016a). “Effect of Superabsorbent Polymers (SAP) on Fresh
425 State Mortars with Ground Granulated Blast-Furnace Slag (GGBS).” *5th International
426 Conference on the Durability of Concrete Structures*, Shenzhen.

427 Almeida, F. C. R., and Klemm, A. J. (2016b). “Evaluation of hardened state properties of GGBS-PC
428 mortars modified by superabsorbent polymers (SAP).” *International RILEM Conference on
429 Materials, Systems and Structures in Civil Engineering*, Lyngby, 11–20.

430 Almeida, F. C. R., and Klemm, A. J. (2017). “Microstructure alteration of PC-GGBS mortars by
431 superabsorbent polymers (SAP).” *14th International Conference on Durability of Building
432 Materials and Components*, PRO 113, Ghent, 205–216.

433 Almeida, F. C. R., and Klemm, A. J. (2018). “Efficiency of internal curing by superabsorbent
434 polymers (SAP) in PC-GGBS mortars.” *Cement and Concrete Composites*, 88, 41–51.

435 Almeida, F. C. R., Sales, A., Moretti, J. P., and Mendes, P. C. D. (2015). “Sugarcane bagasse ash sand
436 (SBAS): Brazilian agroindustrial by-product for use in mortar.” *Construction and Building
437 Materials*, Elsevier Ltd, 82, 31–38.

438 Beushausen, H., Gillmer, M., and Alexander, M. (2014). “The influence of superabsorbent polymers
439 on strength and durability properties of blended cement mortars.” *Cement and Concrete
440 Composites*, Elsevier Ltd, 52, 73–80.

441 Bouasker, M., Khalifa, N. E. H., Mounanga, P., and Ben Kahla, N. (2014). “Early-age deformation
442 and autogenous cracking risk of slag–limestone filler-cement blended binders.” *Construction
443 and Building Materials*, 55, 158–167.

444 Brandt, N. N., Chikishev, A. Y., and Kruzhilin, V. N. (2017). “Raman study of the cleavage of

445 disulphide bonds in albumin, chymotrypsin, and thrombin.” *Vibrational Spectroscopy*, Elsevier
446 B.V., 89, 75–80.

447 BS EN 1015-11. (2006). “Methods of Test for Mortar for Masonry - Part 11: Determination of
448 Flexural and Compressive Strength of Hardened Mortar.” *British Standard*.

449 BS EN 1015-3. (2006). “Methods of Test for Mortar for Masonry - Part 3: Determination of
450 consistence of fresh mortar (by flow table).” *British Standard*.

451 BS EN 15167-1. (2006). “Ground granulated blast furnace slag for use in concrete , mortar and grout -
452 Part 1: Definitions, specifications and conformity criteria.” *British Standard*.

453 BS EN 197-1. (2011). “Cement Part 1: Composition, Specifications and Conformity Criteria for
454 Common Cements.” *British Standard*, 50.

455 Chu, M., Zhu, S.-Q., Huang, Z.-B., and Li, H.-M. (2008). “Influence of Potassium Humate on the
456 Swelling Properties of a Poly(acrylic acid-co-acrylamide)/ Potassium Humate Superabsorbent
457 Composite.” *Journal of Applied Polymer Science*, 107, 3727–3733.

458 Damineli, B. L., Kemeid, F. M., Aguiar, P. S., and John, V. M. (2010). “Measuring the eco-efficiency
459 of cement use.” *Cement and Concrete Composites*, Elsevier Ltd, 32(8), 555–562.

460 Dho, S. K., and Choi, C. H. (1995). “Effects of divalent cations on alkaline hydrolysis of
461 poly(ethylene terephthalate) fabric.” *Journal of the Korea Society of Dyers and Finishers*, 7(4),
462 61–73.

463 Divsholi, B. S., Lim, T. Y. D., and Teng, S. (2014). “Durability Properties and Microstructure of
464 Ground Granulated Blast Furnace Slag Cement Concrete.” *International Journal of Concrete
465 Structures and Materials*, 8(2), 157–164.

466 Esteves, L. P. (2010). “On the absorption kinetics of superabsorbent polymers.” *International RILEM
467 Conference on Use of Superabsorbent Polymers and Other New Additives in Concrete*, RILEM,
468 Lyngby, 77–84.

469 Fairbairn, E. M. R., Americano, B. B., Cordeiro, G. C., Paula, T. P., Toledo Filho, R. D., and Silvano,

470 M. M. (2010). "Cement replacement by sugar cane bagasse ash: CO₂ emissions reduction and
471 potential for carbon credits." *Journal of Environmental Management*, 91(9), 1864–1871.

472 Farzanian, K., and Ghahremaninezhad, A. (2017). "The effect of the capillary forces on the desorption
473 of hydrogels in contact with a porous cementitious material." *Materials and
474 Structures/Materiaux et Constructions*, Springer Netherlands, 50(5), 1–15.

475 Farzanian, K., Pimenta Teixeira, K., Perdigão Rocha, I., De Sa Carneiro, L., and Ghahremaninezhad,
476 A. (2016). "The mechanical strength, degree of hydration, and electrical resistivity of cement
477 pastes modified with superabsorbent polymers." *Construction and Building Materials*, Elsevier
478 Ltd, 109, 156–165.

479 Filho, R. D. T., Silva, E. F., Lopes, A. N. M., Mechtcherine, V., and Dudziak, L. (2012). "Effect of
480 Superabsorbent Polymers on the Workability of Concrete and Mortar." *Application of Super
481 Absorbent Polymers (SAP) in Concrete Construction: State-of-the-Art Report Prepared by
482 Technical Committee 225-SAP*, V. Mechtcherine and H.-W. Reinhardt, eds., Springer
483 Netherlands, Dordrecht, 39–50.

484 Flory, P. J., and Rehner, J. (1943). "Statistical Mechanics of Cross-Linked Polymer Networks II.
485 Swelling." *The Journal of Chemical Physics*, American Institute of Physics, 11(11), 521–526.

486 Flower, D. J. M., and Sanjayan, J. G. (2007). "Green house gas emissions due to concrete
487 manufacture." *International Journal of Life Cycle Assessment*, 12(5), 282–288.

488 Ghourchian, S., Wyrzykowski, M., Baquerizo, L., and Lura, P. (2018). "Susceptibility of Portland
489 cement and blended cement concretes to plastic shrinkage cracking." *Cement and Concrete
490 Composites*, Elsevier Ltd, 85, 44–55.

491 Hasholt, M. T., Jensen, O. M., Kovler, K., and Zhutovsky, S. (2012). "Can superabsorbent polymers
492 mitigate autogenous shrinkage of internally cured concrete without compromising the strength?"
493 *Construction and Building Materials*, 31, 226–230.

494 Hooton, R. D. (2008). "Bridging the gap between research and standards." *Cement and Concrete
495 Research*, 38(2), 247–258.

496 Horie, K., Báron, M., Fox, R. B., He, J., Hess, M., Kahovec, J., Kitayama, T., Kubisa, P., Maréchal,
497 E., Mormann, W., Stepto, R. F. T., Tabak, D., Vohlídal, J., Wilks, E. S., and Work, W. J. (2004).
498 “Definitions of terms relating to reactions of polymers and to functional polymeric materials
499 (IUPAC Recommendations 2003).” *Pure and Applied Chemistry*, 76(4), 889–906.

500 Huang, L., Krigsvoll, G., Johansen, F., Liu, Y., and Zhang, X. (2018). “Carbon emission of global
501 construction sector.” *Renewable and Sustainable Energy Reviews*, Elsevier Ltd, 81(June 2017),
502 1906–1916.

503 Jensen, O. M., and Hansen, P. F. (2001). “Water-entrained cement-based materials: I. Principles and
504 theoretical background.” *Cement and Concrete Research*, 31(4), 647–654.

505 Jensen, O. M., and Hansen, P. F. (2002). “Water-entrained cement-based materials: II. Experimental
506 observations.” *Cement and Concrete Research*, 32, 973–978.

507 Jiang, C., Yang, Y., Wang, Y., Zhou, Y., and Ma, C. (2014). “Autogenous shrinkage of high
508 performance concrete containing mineral admixtures under different curing temperatures.”
509 *Construction and Building Materials*, 61, 260–269.

510 John, V. M., and Zordan, S. E. (2001). “Research and development methodology for recycling
511 residues as building materials - A proposal.” *Waste Management*, 21(3), 213–219.

512 Kang, S. H., Hong, S. G., and Moon, J. (2017). “Absorption kinetics of superabsorbent polymers
513 (SAP) in various cement-based solutions.” *Cement and Concrete Research*, Elsevier Ltd, 97,
514 73–83.

515 Klemczak, B., and Batog, M. (2016). “Heat of hydration of low-clinker cements: Part I. Semi-
516 adiabatic and isothermal tests at different temperature.” *Journal of Thermal Analysis and*
517 *Calorimetry*, Springer Netherlands, 123(2), 1351–1360.

518 Klemm, A. J., and Almeida, F. C. R. (2018). “Towards more sustainable construction-application of
519 superabsorbent polymers in cementitious matrices with reduced carbon footprint.” *MATEC Web*
520 *of Conferences*.

521 Krafcik, M. J., and Erk, K. A. (2016). "Characterization of superabsorbent poly (sodium-acrylate
522 acrylamide) hydrogels and influence of chemical structure on internally cured mortar."
523 *Materials and Structures*, Springer Netherlands, 49(11), 4765–4778.

524 Krivenko, P., Drochytka, R., Gelevera, A., and Kavalerova, E. (2014). "Mechanism of preventing the
525 alkali–aggregate reaction in alkali activated cement concretes." *Cement and Concrete*
526 *Composites*, 45, 157–165.

527 Lee, K. M., Lee, H. K., Lee, S. H., and Kim, G. Y. (2006). "Autogenous shrinkage of concrete
528 containing granulated blast-furnace slag." *Cement and Concrete Research*, 36(7), 1279–1285.

529 Li, A., Zhang, J., and Wang, A. (2005). "Synthesis, characterization and water absorbency properties
530 of poly(acrylic acid)/sodium humate superabsorbent composite." *Polymers for Advanced*
531 *Technologies*, 16(9), 675–680.

532 Li, S. (2016). "Microstructure and composition characterisation of three 20-year-old GGBS-OPC
533 blended pastes." *Construction and Building Materials*, Elsevier Ltd, 123, 226–234.

534 Li, Y., Bao, J., and Guo, Y. (2010). "The relationship between autogenous shrinkage and pore
535 structure of cement paste with mineral admixtures." *Construction and Building Materials*,
536 Elsevier Ltd, 24(10), 1855–1860.

537 Loser, R., Lothenbach, B., Leemann, A., and Tuchschnid, M. (2010). "Chloride resistance of
538 concrete and its binding capacity - Comparison between experimental results and
539 thermodynamic modeling." *Cement and Concrete Composites*, Elsevier Ltd, 32(1), 34–42.

540 Lothenbach, B., Le Saout, G., Ben Haha, M., Figi, R., and Wieland, E. (2012). "Hydration of a low-
541 alkali CEM III/B–SiO₂ cement (LAC)." *Cement and Concrete Research*, 42(2), 410–423.

542 Lothenbach, B., Scrivener, K., and Hooton, R. D. (2011). "Supplementary cementitious materials."
543 *Cement and Concrete Research*, 41(12), 1244–1256.

544 Lura, P., van Breugel, K., and Maruyama, I. (2001). "Effect of curing temperature and type of cement
545 on early-age shrinkage of high-performance concrete." *Cement and Concrete Research*, 31(12),

546 1867–1872.

547 Mechtcherine, V., Gorges, M., Schroefl, C., Assmann, A., Brameshuber, W., Ribeiro, A. B., Cusson,
548 D., Custódio, J., Silva, E. F., Ichimiya, K., Igarashi, S., Klemm, A., Kovler, K., Mendonça
549 Lopes, A. N., Lura, P., Nguyen, V. T., Reinhardt, H.-W., Filho, R. D. T., Weiss, J.,
550 Wyrzykowski, M., Ye, G., and Zhutovsky, S. (2013). “Effect of internal curing by using
551 superabsorbent polymers (SAP) on autogenous shrinkage and other properties of a high-
552 performance fine-grained concrete: results of a RILEM round-robin test.” *Materials and*
553 *Structures*, 47(3), 541–562.

554 Mechtcherine, V., and Reinhardt, H.-W. (Eds.). (2012). *Application of Superabsorbent Polymers (*
555 *SAP) in Concrete Construction: State-of-the-Art Report Prepared by Technical Committee 225-*
556 *SAP*. Springer, RILEM.

557 Mechtcherine, V., Secrieru, E., and Schröfl, C. (2015). “Effect of superabsorbent polymers (SAPs) on
558 rheological properties of fresh cement-based mortars — Development of yield stress and plastic
559 viscosity over time.” *Cement and Concrete Research*, 67, 52–65.

560 Mechtcherine, V., Snoeck, D., Schröfl, C., De Belie, N., Klemm, A. J., Ichimiya, K., Moon, J.,
561 Wyrzykowski, M., Lura, P., Toropovs, N., Assmann, A., Igarashi, S., De La Varga, I., Almeida,
562 F. C. R., Erk, K., Ribeiro, A. B., Custódio, J., Reinhardt, H. W., and Falikman, V. (2018).
563 “Testing superabsorbent polymer (SAP) sorption properties prior to implementation in concrete:
564 results of a RILEM Round-Robin Test.” *Materials and Structures*, 51(1), 28.

565 Mignon, A., Graulus, G. J., Snoeck, D., Martins, J., De Belie, N., Dubruel, P., and Van Vlierberghe,
566 S. (2014). “pH-sensitive superabsorbent polymers: a potential candidate material for self-healing
567 concrete.” *Journal of Materials Science*, 50(2), 970–979.

568 Mignon, A., Snoeck, D., Dubruel, P., Vlierberghe, S. Van, and De Belie, N. (2017). “Crack mitigation
569 in concrete: Superabsorbent polymers as key to success?” *Materials*, 10(3).

570 Mignon, A., Snoeck, D., Schaubroeck, D., Luickx, N., Dubruel, P., Van Vlierberghe, S., and De
571 Belie, N. (2015). “pH-responsive superabsorbent polymers: A pathway to self-healing of

572 mortar.” *Reactive and Functional Polymers*, 93, 68–76.

573 Moretti, J. P., Sales, A., Quarcioni, V. A., Silva, D. C. B., Oliveira, M. C. B., Pinto, N. S., and Ramos,
574 L. W. S. L. (2018). “Pore size distribution of mortars produced with agroindustrial waste.”
575 *Journal of Cleaner Production*, Elsevier Ltd.

576 Pacheco-Torgal, F., Jalali, S., Labrincha, J., and John, V. M. (Eds.). (2013). *Eco-Efficient Concrete*.
577 Woodhead Publishing Ltd.

578 Pourjavadi, A., Fakoorpoor, S. M., Hosseini, P., and Khaloo, A. (2013). “Interactions between
579 superabsorbent polymers and cement-based composites incorporating colloidal silica
580 nanoparticles.” *Cement and Concrete Composites*, 37, 196–204.

581 Provis, J. L. (2014). “Geopolymers and other alkali activated materials: why, how, and what?”
582 *Materials and Structures*, 47, 11–25.

583 Rodrigues, F. A., and Joekes, I. (2011). “Cement industry: Sustainability, challenges and
584 perspectives.” *Environmental Chemistry Letters*, 9(2), 151–166.

585 Sales, A., and Lima, S. A. (2010). “Use of Brazilian sugarcane bagasse ash in concrete as sand
586 replacement.” *Waste Management*, 30(6), 1114–1122.

587 Schroefl, C., Mechtcherine, V., Vontobel, P., Hovind, J., and Lehmann, E. (2015). “Sorption kinetics
588 of superabsorbent polymers (SAPs) in fresh Portland cement-based pastes visualized and
589 quantified by neutron radiography and correlated to the progress of cement hydration.” *Cement
590 and Concrete Research*, 75, 1–13.

591 Schröfl, C., Mechtcherine, V., and Gorges, M. (2012). “Relation between the molecular structure and
592 the efficiency of superabsorbent polymers (SAP) as concrete admixture to mitigate autogenous
593 shrinkage.” *Cement and Concrete Research*, 42(6), 865–873.

594 Schröfl, C., Snoeck, D., and Mechtcherine, V. (2017). “A review of characterisation methods for
595 superabsorbent polymer (SAP) samples to be used in cement-based construction materials:
596 report of the RILEM TC 260-RSC.” *Materials and Structures*, 50(4), 197.

597 Scrivener, K. L., John, V. M., and Gartner, E. M. (2016). *Eco-efficient cements: Potential*
598 *economically viable solutions for a low-CO2 cement- based materials industry. United Nations*
599 *Environment Program, Paris.*

600 Scrivener, K. L., Juilland, P., and Monteiro, P. J. M. (2015a). “Advances in understanding hydration
601 of Portland cement.” *Cement and Concrete Research*, 78, 38–56.

602 Scrivener, K. L., Lothenbach, B., De Belie, N., Gruyaert, E., Skibsted, J., Snellings, R., and
603 Vollpracht, A. (2015b). “TC 238-SCM: hydration and microstructure of concrete with SCMs.”
604 *Materials and Structures*, 48(4), 835–862.

605 Shen, D., Wang, X., Cheng, D., Zhang, J., and Jiang, G. (2016). “Effect of internal curing with super
606 absorbent polymers on autogenous shrinkage of concrete at early age.” *Construction and*
607 *Building Materials*, 106, 512–522.

608 Siddique, R. (2014). “Utilization (recycling) of iron and steel industry by-product (GGBS) in
609 concrete: Strength and durability properties.” *Journal of Material Cycles and Waste*
610 *Management*, 16(3), 460–467.

611 Siddique, R., and Bennacer, R. (2012). “Use of iron and steel industry by-product (GGBS) in cement
612 paste and mortar.” *Resources, Conservation and Recycling*, 69, 29–34.

613 Sikora, K. S., and Klemm, A. J. (2015). “Effect of Superabsorbent Polymers on Workability and
614 Hydration Process in Fly Ash Cementitious Composites.” *Journal of Materials in Civil*
615 *Engineering*, American Society of Civil Engineers, 27(5), 4014170.

616 Siritwatwechakul, W., Siramanont, J., and Vichit-Vadakan, W. (2012). “Behavior of Superabsorbent
617 Polymers in Calcium- and Sodium-Rich Solutions.” *Journal of Materials in Civil Engineering*,
618 24(8), 976–980.

619 Snoeck, D., Jensen, O. M., and De Belie, N. (2015). “The influence of superabsorbent polymers on
620 the autogenous shrinkage properties of cement pastes with supplementary cementitious
621 materials.” *Cement and Concrete Research*, 74, 59–67.

622 Snoeck, D., Schaubroeck, D., Dubruel, P., and De Belie, N. (2014a). "Effect of high amounts of
623 superabsorbent polymers and additional water on the workability, microstructure and strength of
624 mortars with a water-to-cement ratio of 0.50." *Construction and Building Materials*, 72, 148–
625 157.

626 Snoeck, D., Tittelboom, K. V., Steuperaert, S., Dubruel, P., and Belie, N. D. (2014b). "Self-healing
627 cementitious materials by the combination of microfibres and superabsorbent polymers."
628 *Journal of Intelligent Material Systems and Structures*, 25(1), 13–24.

629 Tachibana, Y., Baba, T., and Kasuya, K. (2017). "Environmental biodegradation control of polymers
630 by cleavage of disulfide bonds." *Polymer Degradation and Stability*, Elsevier Ltd, 137, 67–74.

631 Tazawa, E., and Miyazawa, S. (1995). "Influence of cement and admixture on autogenous shrinkage
632 of cement paste." *Cement and Concrete Research*, 25(2), 281–287.

633 Thomas, M. (2011). "The effect of supplementary cementing materials on alkali-silica reaction: A
634 review." *Cement and Concrete Research*, 41(12), 1224–1231.

635 Valcuende, M., Benito, F., Parra, C., and Miñano, I. (2015). "Shrinkage of self-compacting concrete
636 made with blast furnace slag as fine aggregate." *Construction and Building Materials*, 76, 1–9.

637 Visakh, P. M., Bayraktar, O., and Pico, G. A. (Eds.). (2014). *Polyelectrolytes: Thermodynamics and*
638 *Rheology. Polyelectrolytes: Thermodynamics and Rheology*, Springer.

639 Vollpracht, A., Lothenbach, B., Snellings, R., and Haufe, J. (2016). "The pore solution of blended
640 cements: a review." *Materials and Structures*, 49(8), 3341–3367.

641 Wehbe, Y., and Ghahremaninezhad, A. (2017). "Combined effect of shrinkage reducing admixtures
642 (SRA) and superabsorbent polymers (SAP) on the autogenous shrinkage, hydration and
643 properties of cementitious materials." *Construction and Building Materials*, 138, 151–162.

644 Zhu, Q., Barney, C. W., and Erk, K. A. (2015). "Effect of ionic crosslinking on the swelling and
645 mechanical response of model superabsorbent polymer hydrogels for internally cured concrete."
646 *Materials and Structures*, Springer Netherlands, 48(7), 2261–2276.

Table 1. Chemical and physical characterization of PC and GGBS

Parameter	Unit	PC	GGBS
CaO	wt%	62.44	38.53
SiO ₂	wt%	20.07	34.53
Al ₂ O ₃	wt%	4.85	13.4
MgO	wt%	2.20	9.74
TiO ₂	wt%	-	0.82
Fe ₂ O ₃	wt%	2.72	0.21
SO ₃	wt%	3.15	0.35
Na ₂ O	wt%	0.31	0.17
K ₂ O	wt%	0.62	0.59
MnO	wt%	-	0.22
Cl ⁻	wt%	0.06	0.02
LOI	wt%	2.77	0.64
Bulk density	kg/L	1.28	1.11
Specific surface	m ² /kg	410	390

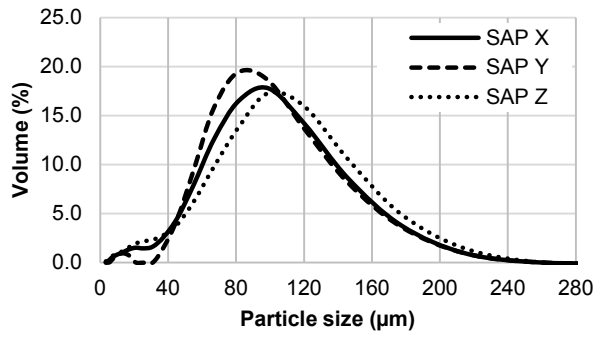
Table 2. Mix compositions of mortars

Sample name	Type of SAP	PC content (%)	GGBS content (%)	Mass of materials (g)				
				PC	GGBS	SAP	Sand	Water
R0	-	100%	0%	587.0	-	-	1174.0	293.5
X0	SAP X	100%	0%	587.0	-	1.5	1174.0	293.5
Y0	SAP Y	100%	0%	587.0	-	1.5	1174.0	293.5
Z0	SAP Z	100%	0%	587.0	-	1.5	1174.0	293.5
R75	-	25%	75%	146.8	440.3	-	1174.0	293.5
X75	SAP X	25%	75%	146.8	440.3	1.5	1174.0	293.5
Y75	SAP Y	25%	75%	146.8	440.3	1.5	1174.0	293.5
Z75	SAP Z	25%	75%	146.8	440.3	1.5	1174.0	293.5

Table 3. Chemical composition of the studied SAPs by EDX analysis (by wt%)

Elements	SAP X		SAP Y		SAP Z	
	Average	SD	Average	SD	Average	SD
C	49.8	1.8	47.3	1.6	46.9	0.8
O	28.2	1.0	30.8	0.5	29.3	0.5
N	12.7	0.4	11.0	0.7	11.2	0.8
K	0.0	0.0	3.2	0.3	12.0	1.3
Na	4.0	0.3	5.7	0.5	0.2	0.1
S	5.3	0.5	2.1	0.2	0.3	0.1

Note: SD = standard deviation



		SAP X	SAP Y	SAP Z
d(v,0.5)	μm	84.88	85.13	89.55
d(v,0.1)	μm	32.96	49.72	26.01
mode	μm	95.19	85.74	102.51
d(v,0.9)	μm	140.00	139.64	147.24

Fig. 1. Particle size distribution of the studied SAPs

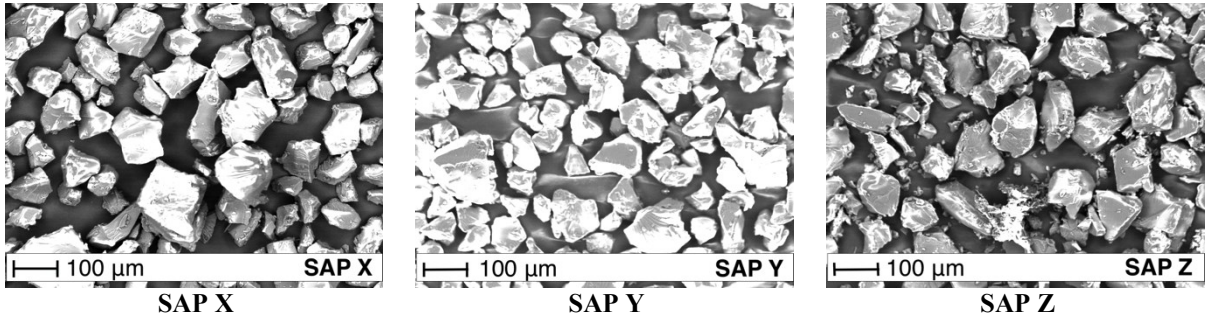


Fig. 2. The SEM micrographs of the studied SAPs

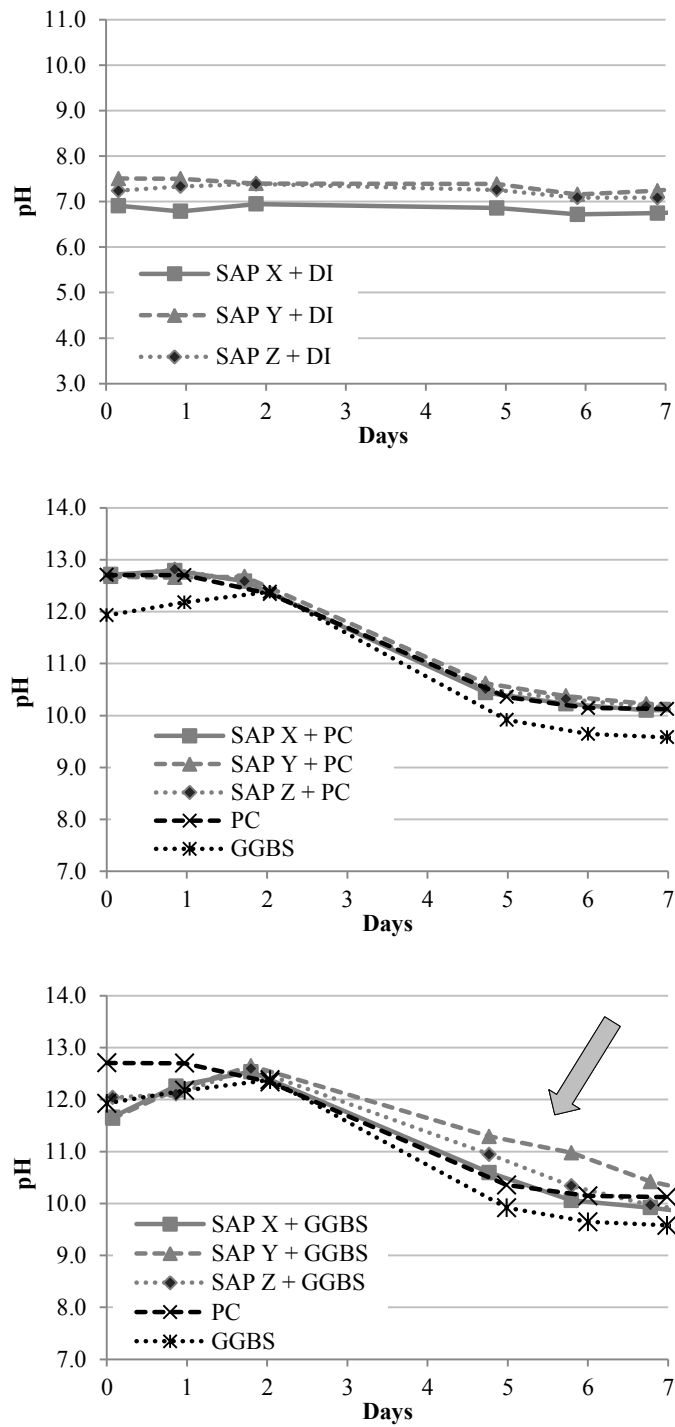


Fig. 3. pH analysis of SAP solutions in deionised water (DI), PC and GGBS filtrates

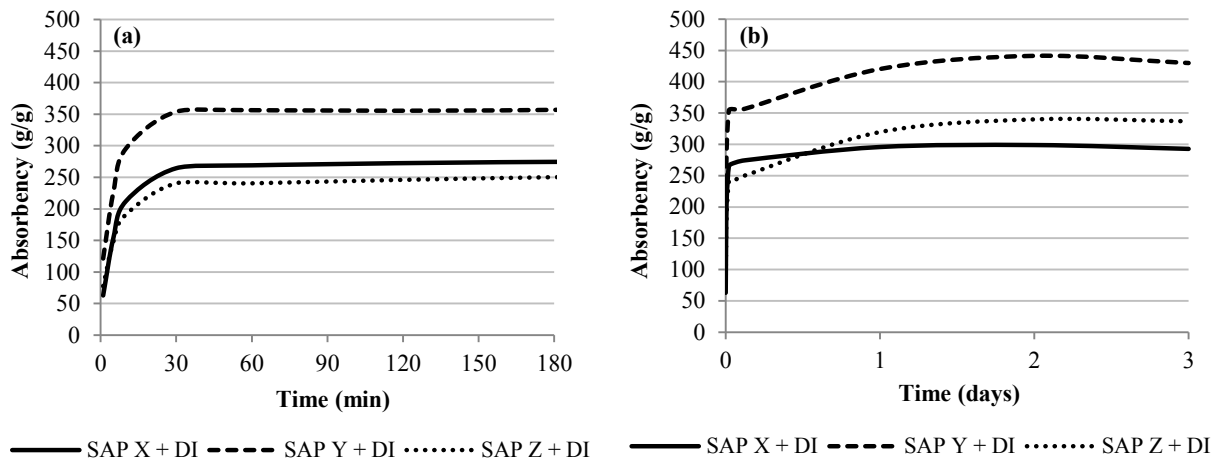


Fig. 4. Sorption behaviour of SAPs in DI water: (a) up to 180 min; (b) up to 3 days

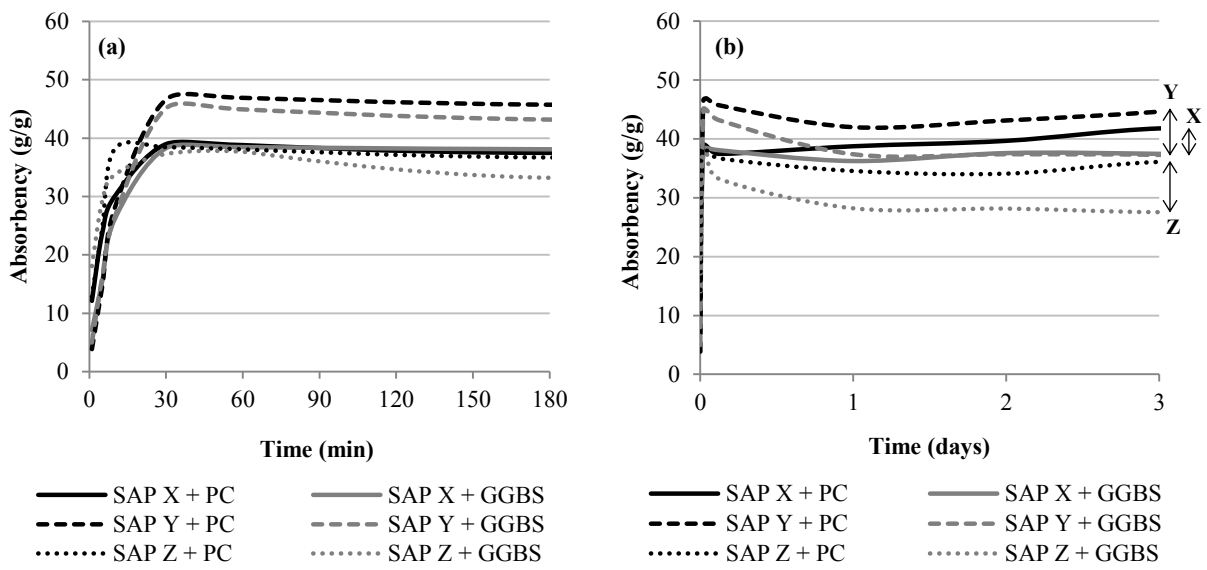


Fig. 5. Sorption behaviour of SAPs in cementitious solutions: (a) up to 180 min; (b) right: up to 3 days. Arrows in graph (b) indicate the difference between absorbency in PC and GGBS systems for all SAPs

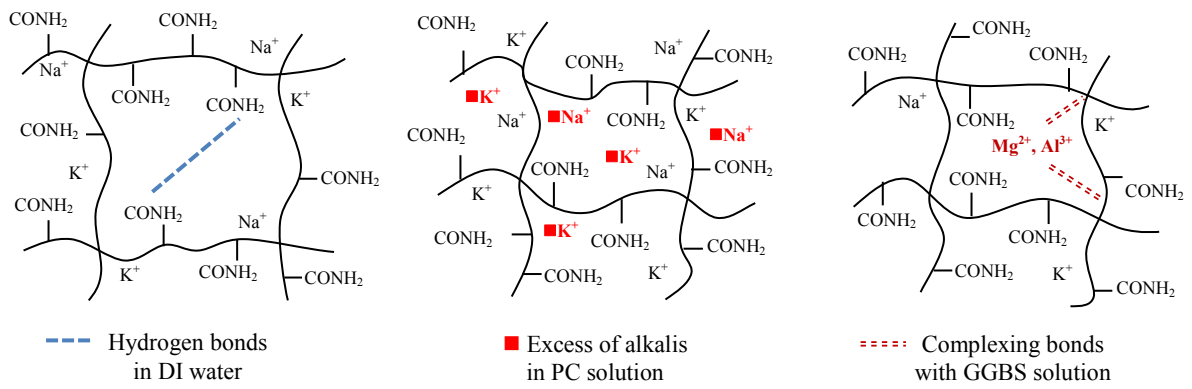


Fig. 6. Polyacrylamide structures and their modifications (adapted from Chu et al. 2008)

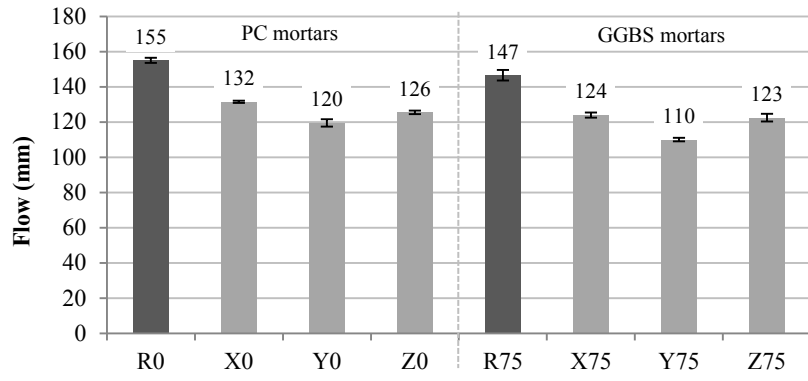


Fig. 7. Flow-table results of PC-GGBS mortars modified by SAPs

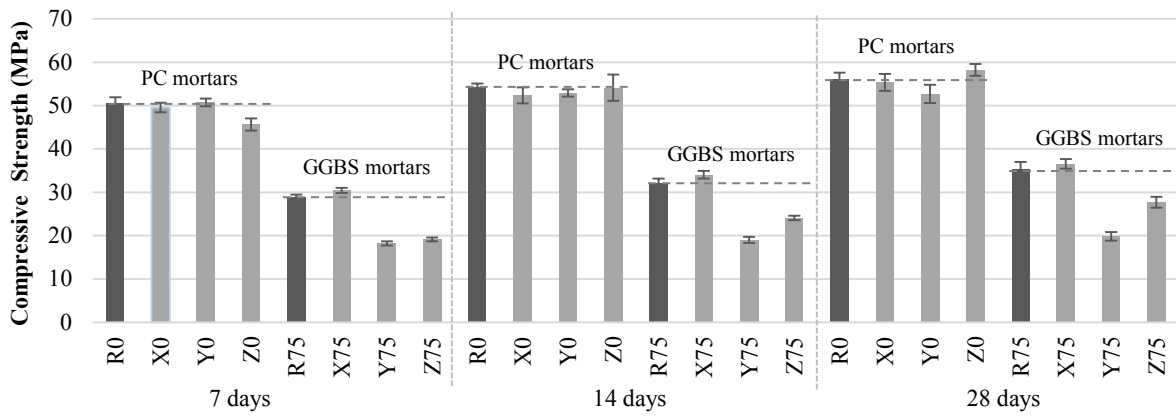


Fig. 8. Compressive strength results of PC-GGBS mortars modified by SAPs

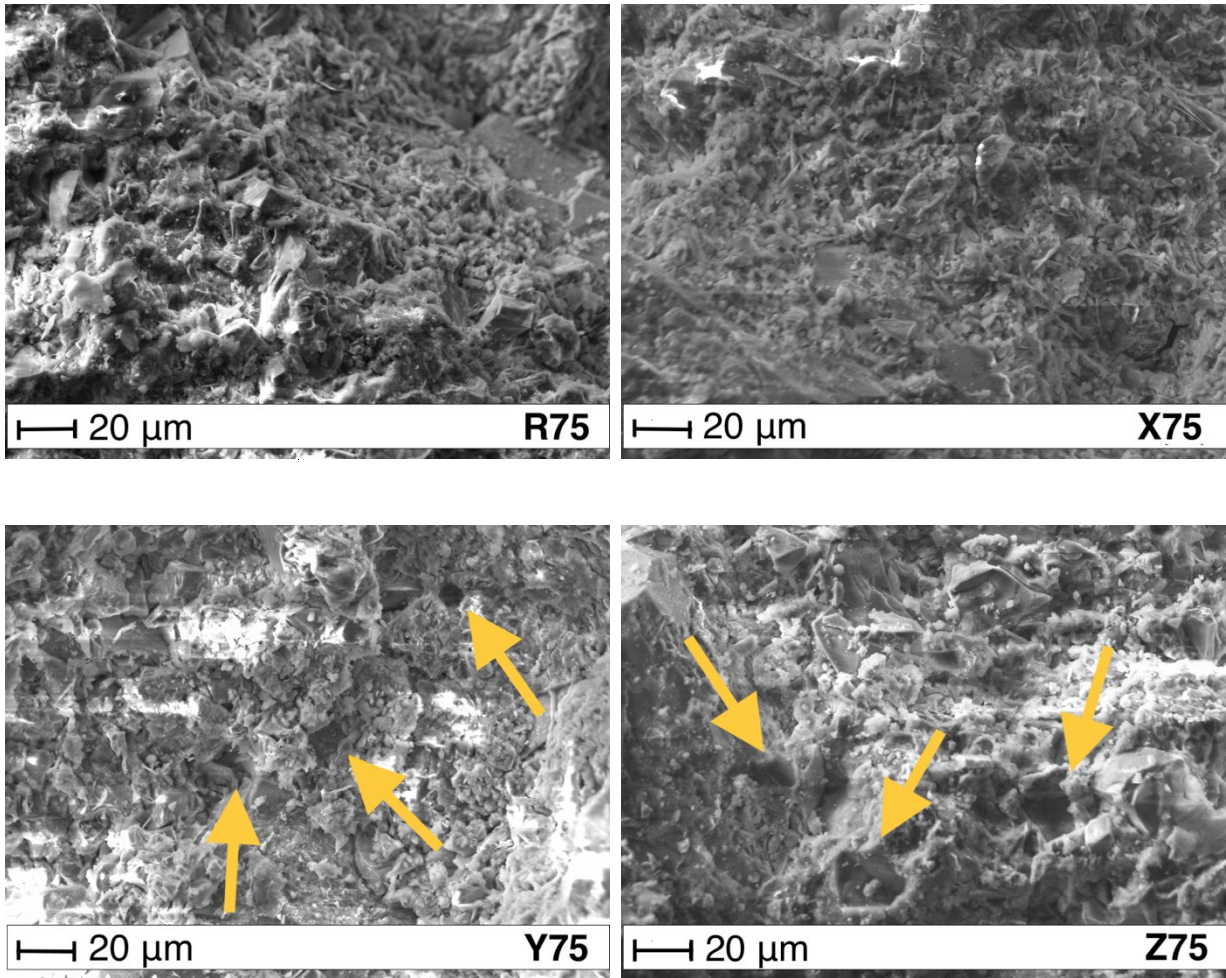


Fig. 9. SEM micrographs of GGBS mortars at 28 days (indication of larger pores in samples modified by SAP Y and SAP Z)

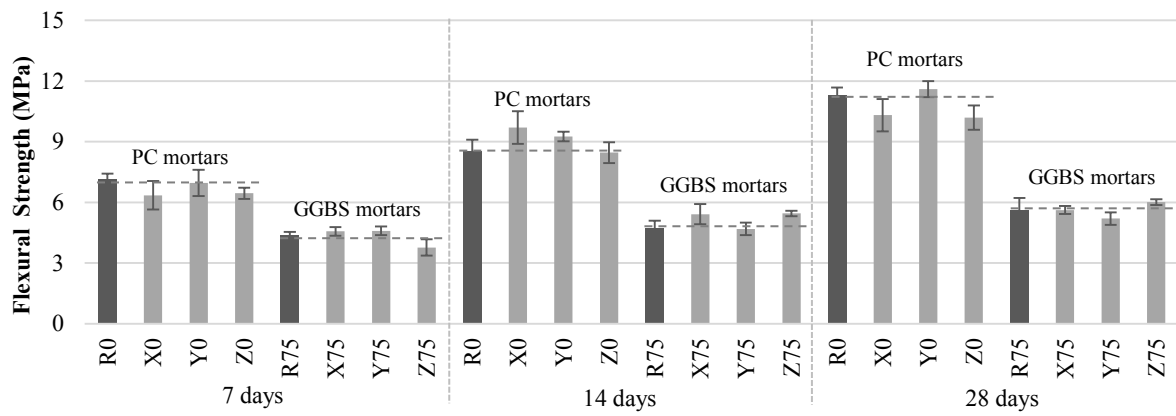


Fig. 10. Flexural strength results of PC-GGBS mortars modified by SAPs